

# TRUNCATION IN BEAM WAVEGUIDES

J. Anthony Murphy,  
Maynooth College, Co. Kildare, Ireland

Stafford Withington,  
Cavendish Laboratory, University of Cambridge, CB3 0HE, England

## Abstract

We present a technique for determining the power loss and diffraction effects that occur when the field in a beam waveguide is truncated by an axially symmetric stop. The technique is based on the principles of multimode Gaussian optics. Although the underlying theory is applicable to any long-focal-length optical system, we concentrate on beam waveguides that are fed by diagonal horns, corrugated horns, smooth-walled conical horns, and uniformly illuminated apertures. We demonstrate the technique by calculating the total loss and beam profiles in a system comprising a diagonal horn, a lens, a window, and two off-axis mirrors, with the finite size of each component taken into account.

## 1 INTRODUCTION

When designing the quasi-optical systems of millimetre and submillimetre-wave receivers, it is necessary to know at what radius the propagating beam can be truncated at a stop or aperture without incurring a significant loss. If the beam has been refocussed a number of times, perhaps by a series of lenses or mirrors, the loss cannot be calculated by simply integrating the far-field pattern of the feed antenna over the region defined by the stop. Also, if the beam is significantly truncated diffraction effects will occur, which will affect the subsequent behaviour of the beam.

To first order, a known field can be traced through a long-focal-length optical system by extracting the lowest-order Gaussian mode [1]. In the case of a corrugated horn, this approach is particularly attractive, since the field at the mouth of the horn is linearly polarized and can be described as a simple Gaussian to high accuracy [2]. However, for a diagonal or smooth-walled conical horn, or indeed any antenna that does not have a Gaussian aperture distribution, the situation is more complicated, because, although the simple Gaussian gives an indication of how the scale size of the beam changes as one moves through the optical system, it does not give any indication of how the sidelobe structure of the beam evolves [3] [4], [5]. This limitation is particularly troublesome when the illuminating antenna has a

highly-truncated aperture field, because then the beam changes from being spatially confined to being spatially diffuse as one moves in and out of foci. In the single-mode approximation one is therefore left with the problem of surmising how the  $1/e$  Gaussian radius is related to the poorly-defined radial edge of the actual beam.

To solve this problem higher-order modes can be introduced into the theoretical description of the propagating field. (e.g. [6], [2], [7], [3]). We have devised a straightforward technique for determining the power loss, which is based on the idea that for a multimode Gaussian beam the scale size of the beam at a plane is characterised by the Gaussian radius and the sidelobe structure of the beam is characterised by the phase slippage; hence the truncation loss is completely determined by these two quantities. It is therefore possible, for axially symmetric truncation of the beam, to summarise the results for a particular feed antenna in a single contour plot, which shows truncation loss as a function of normalised aperture size and phase slippage. We discuss how such a plot can be used together with single-mode design techniques to minimise the size of millimetre and submillimetre-wave optical systems. If diffraction effects do occur due to significant beam truncation, then these can be conveniently analysed using scattering matrix theory applied to Gaussian beam modes [8], [9]. We illustrate the approach by calculating the beam profiles in a system comprising a diagonal horn, a lens, a window and two off-axis mirrors, where the finite size of each component is taken into account.

## 2 APERTURE-FIELD EXPANSIONS

### 2.1 Associated Laguerre modes

For a circular stop that is coaxial with the direction of propagation and perfectly absorbing outside the transmitting region, the propagating fields are most conveniently described as a sum of Associated Laguerre-Gaussian modes defined by:

$$\psi_n^{\alpha, \cos/\sin}(r, \theta, z) = \sqrt{\frac{2(2 - \delta_{0n})n!}{\pi W^2(n + \alpha)!}} \left[2\left(\frac{r}{W}\right)^2\right]^{\frac{\alpha}{2}} L_n^\alpha \left[2\left(\frac{r}{W}\right)^2\right] \exp\left[-\left(\frac{r}{W}\right)^2\right] \exp\left[-jk\left(z + \frac{r^2}{2R}\right) + j(2n + \alpha + 1)\phi_0\right] \begin{cases} \cos(\alpha\theta) \\ \sin(\alpha\theta) \end{cases}. \quad (1)$$

The associated Laguerre polynomials are defined as in [10].  $\alpha$  is an integer.  $W$  and  $R$  have their usual significance and  $\phi_0(z) = \tan^{-1}(\pi W^2/\lambda R)$  is the phase slippage for the fundamental mode between the waist and the plane of interest [11]. Notice that the Associated Laguerre polynomials are defined such that the generalised power in each mode  $\iint |\psi_n^\alpha(r, \theta)|^2 r dr d\theta$  is unity.

We can expand the co-polar and cross-polar components of a beam in the form

$$\psi(r, \theta, z) = \sum_{n=0}^{\infty} \sum_{\alpha=0}^{\infty} A_{n\alpha}^c \psi_n^{\alpha, \cos}(r, \theta, z) + A_{n\alpha}^s \psi_n^{\alpha, \sin}(r, \theta, z), \quad (2)$$

where it is understood that the  $A_{0,\alpha}^s$  are all zero. In reality, we truncate the series once the power in the sum is close to 100 % of that in the actual beam. To determine the mode coefficients  $A_{n\alpha}^{c/s}$ , we evaluate the overlap integrals at the aperture of the horn. If the length of the horn is  $L$ , the field at the aperture can be written

$$\psi(r, \theta) = \begin{cases} \psi_h(r, \theta) \exp[-jk\tau^2/2L] & \text{for } r < a \\ 0 & \text{otherwise} \end{cases}. \quad (3)$$

On setting the common-mode radius of curvature equal to the length, we can determine  $A_{n\alpha}^{c/s}$  through

$$A_{n\alpha}^{c/s} = e^{j\beta_{n\alpha}} \int \int_A r dr d\theta \psi_h(r, \theta) \sqrt{\frac{n!2(2-\delta_{n0})}{(n+\alpha)! \pi W_h^2}} \left[ 2 \left( \frac{r}{W_h} \right)^2 \right]^{\frac{\alpha}{2}} L_n^\alpha \left( 2 \left( \frac{r}{W_h} \right)^2 \right) \exp \left[ - \left( \frac{r}{W_h} \right)^2 \right] \begin{cases} \cos(\alpha\theta) \\ \sin(\alpha\theta) \end{cases} \quad (4)$$

where  $\beta_{n\alpha} = kz_h - j(2n + \alpha + 1)\phi_o(z_h)$ . In these equations  $W_h$  is the Gaussian radius at the aperture, and  $z_h$  is the position of the aperture with respect to the virtual waist [2]. It is normal to include the phase factors  $\exp(j\beta_{n\alpha})$  in the mode coefficients, since they depend only on  $z$ .

There is a complete set of orthonormal modes associated with every value of  $W_h$ , and so we are free to choose  $W_h$  in whatever way we wish. It has become common practice to use the value of  $W_h$  that maximises the power in the lowest order mode: we will call this value  $W_{h,opt}$ . It can be shown, however, that in general  $W_{h,opt}$  does not lead to a mode set that is particularly good at sampling the aperture field. In this paper, where we are interested in accurate loss calculations, we will use the value of  $W_h$  that maximises the power in a finite number of modes [12]. Once the contour plot has been generated for this mode set, we can then transform back to the more commonly-used mode set for design purposes.

Let us now consider how the mode coefficients can be calculated for each of the horns of interest.

## 2.2 Corrugated conical horn

The field at the mouth of a moderately-flared corrugated horn operating under balanced-hybrid conditions can be regarded as having an  $HE_{11}$  amplitude distribution with a quadratic phase error:

$$\mathbf{E}_h(r, \theta) \propto J_0(\chi_{cc}r/a) \mathbf{j} \exp[-jkr^2/2L] \quad (5)$$

where  $L$  is the length of the horn,  $a$  is the radius of the aperture, and  $\chi_{cc} = 2.405$ . As described, the field is polarised in the  $y$ -direction, and all of the power is contained in the

symmetric ( $\theta$ -independent) co-polarised component. Thus, only ALG modes of order 0 are required in order to describe the beam. Wylde [2] has shown that for a corrugated horn  $W_{h,opt} = 0.644a$ .

### 2.3 Smooth-walled conical horn

The modal expansion of the smooth-walled conical horn has been discussed by Murphy [4]. The field at the aperture can be regarded as having a  $TE_{11}$  amplitude distribution with a quadratic phase error:

$$\mathbf{E}_h(r, \theta) \propto [(J_0(\chi_{sc}r/a) + J_2(\chi_{sc}r/a) \cos 2\theta)\mathbf{j} + J_2(\chi_{sc}r/a) \sin(2\theta)\mathbf{i}] \exp[-jkr^2/2L] \quad (6)$$

where  $L$  is the length of the horn,  $a$  is the radius of the aperture, and  $\chi_{sc} = 1.841$ . It can be shown that 91.8% of the power lies in the  $\theta$ -independent co-polar component, while 4.1% of the power lies in each of the  $\theta$ -dependent co-polar and cross-polar components. Fortunately, we only need modes of order  $\alpha = 0$  and 2 [4], since all of the field terms are either  $\theta$ -independent, or else depend on  $\cos(2\theta)$  or  $\sin(2\theta)$ . Consequently,

$$\mathbf{E}_h = \sum_{n=0}^{\infty} A_{n0}^c \psi_n^{0,cos}(r, \theta, z_h)\mathbf{j} + A_{n2}^c (\psi_n^{2,cos}(r, \theta, z_h)\mathbf{j} + \psi_n^{2,sin}(r, \theta, z_h)\mathbf{i}), \quad (7)$$

where we have used the fact that  $A_{n2}^c = A_{n2}^s$ . For a conical horn, it can be shown that  $W_{h,opt} = 0.770a$ . When  $W_h = W_{h,opt}$ , and the total number of modes is limited to 200 ( $n_{max} = 100$ ), only 99.3% of the power in the actual beam is included in the expansion. By choosing  $W_h = 0.140a$ , however, this fraction can be increased to 99.6%, and so we have used this value in all of our calculations.

### 2.4 Diagonal horn

The field at the aperture of a moderately-flared diagonal horn supporting spherically-expanding  $TE_{10}$  and  $TE_{01}$  square waveguide modes can be written in the form

$$\mathbf{E}_h(r, \theta) \equiv \mathbf{E}_h(x, y) \propto [\cos(\pi y/a)\mathbf{i} + \cos(\pi x/a)\mathbf{j}] \exp(-jkr^2/2L) \quad (8)$$

where  $L$  is the length of the horn and  $a$  is the sidelength of the aperture. The co-polar direction of the hybrid field can be regarded as the  $\mathbf{v} = \mathbf{i} + \mathbf{j}$  direction, and the cross-polar direction can be regarded as the  $\mathbf{h} = \mathbf{i} - \mathbf{j}$  direction. The field at the aperture can then be written

$$\mathbf{E}_h = \psi_{co}\mathbf{v} + \psi_{cs}\mathbf{h} \quad (9)$$

$$\psi_{co} \propto [\cos(\pi y/a) + \cos(\pi x/a)] \quad (10)$$

$$\psi_{cs} \propto [\cos(\pi y/a) - \cos(\pi x/a)], \quad (11)$$

where  $co, cs$  denote the co-polar and cross-polar components respectively. Withington [5] has already considered the behaviour of diagonal horns in terms of Gaussian modes, but in this

paper we wish to use Laguerre polynomials rather than Hermite polynomials. This slightly more complicated expansion can be achieved by recognising that there is a 4-fold rotational symmetry associated with both the co-polar and the cross-polar fields; therefore

$$\psi_{co}(r, \theta, z) = \sum_{n=0}^{\infty} \sum_{\alpha=0}^{\infty} A_{n(4\alpha)}^c \psi_n^{(4\alpha), \cos}(r, \theta, z) \quad (12)$$

$$\psi_{cs}(r, \theta, z) = \sum_{n=0}^{\infty} \sum_{\alpha=0}^{\infty} A_{n(4\alpha+2)}^s \psi_n^{(4\alpha+2), \sin}(r, \theta, z). \quad (13)$$

The mode coefficients  $A_{n\alpha}, B_{n\alpha}$  can be found by expressing  $r$  and  $\theta$ , in  $\psi_n^\alpha(r, \theta)$ , in terms of  $x$  and  $y$ , and integrating over the aperture. When this Cartesian integration is carried out, it is found that  $W_{h,opt} = 0.430a$ . Furthermore, when  $W_h = W_{h,opt}$ , and the total number of modes is limited to 200 ( $n_{max} = 40, l_{max} = 10$ ), only 98.5% of the power in the actual beam is included in the expansion. By choosing  $W = 0.11a$ , however, this fraction can be increased to 99.1%, and so we have used this value in all of our calculations.

## 2.5 Uniformly-illuminated aperture

The most difficult field to propagate through an optical system is that produced by a uniformly illuminated aperture. Although, of course, one cannot manufacture such a horn, it is precisely this field that would have to pass unimpeded through an optical system if one were trying to maximise the aperture efficiency of a reflecting antenna. It is interesting, therefore, to consider this extreme case.

The beam produced by a uniformly illuminated circular aperture has axial symmetry, and therefore the modal expansion simplifies to a sum of  $\psi_n^0$  ALG modes. If we allow the fields at the aperture, radius  $a$ , to have phase curvature,  $R_h$ , we can write

$$\psi(r) = \begin{cases} \sqrt{\frac{1}{\pi a^2}} \exp[-jkr^2/2R_h] & \text{for } r < a \\ 0 & \text{otherwise} \end{cases} \quad (14)$$

and the mode coefficients become

$$A_{n0}^c(a/W_h) = \frac{2\sqrt{2}}{aW_h} \int_0^a L_n^0(2(r/W_h)^2) \exp[-(r/W_h)^2] r dr. \quad (15)$$

The mode coefficients can be calculated numerically [3], but it is more efficient to use the recursion relationship

$$A_{n+1,0}^c = 2 \frac{(L_n(2(a/W_h)^2) - L_{n+1}(2(a/W_h)^2)) \exp[-(a/W_h)^2]}{\sqrt{2}a/W_h} - A_{n0}^c \quad (16)$$

$$A_{00}^c = 1 - 2 \exp[-(a/W_h)^2]. \quad (17)$$

In the case of a uniformly illuminated aperture, it can be shown that  $W_{h,opt} = 0.892a$ . When  $W_h = W_{h,opt}$ , and the total number of modes is limited to 500, only 98.0% of the power in the actual beam is included in the expansion. If we choose  $W_h = 0.107a$ , however, this fraction can be increased to 99.9%, and so we have used this value in all of our calculations.

### 3 ANALYSIS OF TRUNCATION USING ALG MODES

If a beam is truncated at the plane  $z = z_o$ , by a coaxial circular aperture of radius  $r_t$ , then the field at the aperture has the form  $E_{ap}(r, \theta, z_o) = 0$  for  $r > r_t$ , and we can write for each component of the beam (cross-polar and co-polar):

$$E_{ap}(r, \theta, z_o) = \sum_{n,\alpha} A_{n\alpha}^c \psi_n^{\alpha,cos}(r, \theta, z_o)^T + \sum_{n,\alpha} A_{n\alpha}^s \psi_n^{\alpha,sin}(r, \theta, z_o)^T, \quad (18)$$

where  $T$  denotes a truncated mode. The  $A_{n,\alpha}^{c/s}$  are the mode coefficients for the incident beam. Since a truncated mode is not a true mode of propagation, some of the power in a given incident mode will be redistributed between the other modes. Mathematically, we can write each truncated mode as a sum of true propagating modes:

$$\psi_n^{\alpha,cos}(r, \theta, z_o)^T = \sum_{m,\alpha'} S_{m\alpha',n\alpha}^c \psi_m^{\alpha',cos}(r, \theta, z_o) \text{ and } \psi_n^{\alpha,sin}(r, \theta, z_o)^T = \sum_{m,\alpha'} S_{m\alpha',n\alpha}^s \psi_m^{\alpha',sin}(r, \theta, z_o). \quad (19)$$

Because of the symmetry of the aperture,  $S_{m\alpha',n\alpha}^c$  and  $S_{m\alpha',n\alpha}^s$  are given by

$$S_{m\alpha',n\alpha}^c = S_{m\alpha',n\alpha}^s = \delta_{\alpha\alpha'} I_{m,n}^\alpha \exp[2(n-m)j\phi_o], \quad (20)$$

where

$$I_{m,n}^\alpha(x_t) = \int_0^{x_t} \frac{x^\alpha L_m^\alpha(x) L_n^\alpha(x) e^{-x}}{\sqrt{(m+\alpha)!(n+\alpha)!/m!n!}} dx. \quad (21)$$

and  $x_t = 2(r_t/W)^2$ . The field can then be re-expressed in terms of the propagating modes:

$$E_{ap}(r, \theta, z_o) = \sum_{m,\alpha'} B_{m\alpha'}^c \psi_m^{\alpha',cos}(r, \theta, z_o) + B_{m\alpha'}^s \psi_m^{\alpha',sin}(r, \theta, z_o), \quad (22)$$

where  $B_{m\alpha'}^{c/s} = \sum_{n,\alpha} S_{m\alpha',n\alpha}^{c/s} A_{n\alpha}^{c/s}$ . We can regard  $S_{m\alpha',n\alpha}^{c/s}$  as a scattering matrix, which operates on the vector  $A_{n\alpha}^{c/s}$  of incident mode coefficients to yield the vector  $B_{m\alpha'}^{c/s}$  of transmitted mode coefficients. Thereafter, the beam propagates with the new set of mode coefficients until the next truncating aperture is encountered. Thus, the beam can be reconstructed anywhere along the optical path.

If we are interested in the power that is transmitted through the aperture then this is given by:

$$P_t = \int_{r=0}^{r_t} \int_{\theta=0}^{2\pi} \mathbf{E} \cdot \mathbf{E}^* r dr d\theta = \int_{r=0}^{r_t} \int_{\theta=0}^{2\pi} |\psi_{co}(z)|^2 + |\psi_{cs}(z)|^2 r dr d\theta \quad (23)$$

where  $co$  and  $cs$  denote the co-polar and cross-polar fields respectively. In the following discussion, the co-polar and cross-polar fields  $\psi_{co}, \psi_{cs}$  have been normalised to make the total generalised power  $\int_{r=0}^{\infty} \int_{\theta=0}^{2\pi} \mathbf{E} \cdot \mathbf{E}^* r dr d\theta$  unity. The above equation can be expressed in terms of the phase slippage  $\Delta\phi_o$  between the *aperture of the horn* (where the mode coefficients  $A_{n\alpha}, B_{n\alpha}$  were evaluated) and the plane of interest:

$$(P_t)_{co,cs} = \sum_{m,m,\alpha} (A_{m\alpha}^c A_{n\alpha}^c + A_{m\alpha}^s A_{n\alpha}^s)_{co,cs} I_{m,n}^\alpha(x_t) \exp[2(n-m)j\Delta\phi_o]. \quad (24)$$

The subscripts *co* and *cs* denote the co-polar and cross-polar fields respectively, and the total power transmitted  $P_t$  is the sum of the two components.

It is clear that  $P_t$  depends not only on the ratio of the truncation radius  $r_t$  to the Gaussian beam width  $W(z)$ , but also on the phase slippage  $\Delta\phi_0(z)$ . As stated earlier, the Gaussian radius characterises the scale size of the beam at a plane, and the phase slippage characterises the form (sidelobe structure) of the beam; hence one would expect the fraction of power transmitted to depend on these two quantities.

A key feature of the proposed technique for determining the truncation scattering matrix coefficients and for the truncation power loss calculations is that it is possible to derive recursion relationships for the integrals  $I_{m,n}^\alpha(x_t)$ , which enable the calculations to be evaluated easily. The relationships are:

$$I_{m+1,n+1}^0 = I_{m,n}^0 + (L_m(x_t) - L_{m+1}(x_t))(L_{n+1}(x_t) - L_n(x_t))e^{-x_t} \quad (25)$$

$$\sqrt{\alpha + 1}I_{m,0}^{\alpha+1} = \sqrt{m + \alpha + 1}I_{m,0}^\alpha - \sqrt{m + 1}I_{m+1,0}^\alpha \text{ for } m > 0 \quad (26)$$

$$\sqrt{n + \alpha + 1}I_{m,n}^{\alpha+1} = \sqrt{n}I_{m,n-1}^{\alpha+1} + \sqrt{m + \alpha + 1}I_{m,n}^\alpha - \sqrt{m + 1}I_{m+1,n}^\alpha \text{ for } m, n > 0. \quad (27)$$

For a given plane, the Gaussian radius and the differential phase slippage are functions of the mode set chosen, and so to be precise we should write  $W(z, W_h)$  and  $\Delta\phi_0(z, W_h)$ . For computational reasons, we have used the value of  $W_h$  that maximises the power in a finite number of modes, but from a design point of view, we would like to use the value of  $W_h$  that maximises the power in the lowest-order mode  $W_{h,opt}$ . For every point on the optical path, we therefore need to transform between the computationally convenient  $W = W(z, W_h)$  and  $\phi_0 = \phi_0(z, W_h)$ , and the more commonly used  $W_{opt} = W(z, W_{h,opt})$  and  $\phi_{0,opt} = \phi_0(z, W_{h,opt})$ . After some algebra, it can be shown that

$$\phi_{0,opt} = \arctan((W_h/W_{h,opt})^2 \tan(\phi_0)) \quad (28)$$

$$r_t/W_{opt} = (r_t/W)(W_{h,opt} \sin(\phi_{0,opt})) / (W_h \sin(\phi_0)). \quad (29)$$

Hence, once the contours of constant loss have been calculated, they can be presented in terms of the more commonly used single-mode parameters.

In Figs. 1 - 4 we show, for the diagonal horn, smooth-walled conical horn, corrugated conical horn, and uniformly illuminated aperture, contours of constant loss, as a function of normalised truncation radius  $r_t/W_{opt}$  and differential phase slippage  $\Delta\phi_{0,opt}$ .

It can be seen that for  $\Delta\phi_{0,opt}$  close to zero, the fields are spatially confined, whereas for  $\Delta\phi_{0,opt}$  close to  $\pi/2$ , the fields are diffuse. For a diffraction limited horn, these values correspond to positions in the optical system where there are images of the aperture and Fourier transform of the aperture, respectively. It is important to realise that the central portion of this plot does not necessarily correspond to the beam waist. In fact, in the case of a physically realisable horn, the waist occurs at some negative phase slippage, and the phase slippage only becomes zero once the diverging beam has reached the aperture. As the beam propagates away from the aperture, sidelobe structure develops, and a spatial redistribution of power occurs as the image of the horn undergoes diffraction. This phenomenon shows up as  $P_{tr}$

developing off-axis wings with increasing values of  $\Delta\phi_{0,opt}$ . The majority of the the power still remains within  $r = W_{h,opt}$ , emphasising that the simple Gaussian gives a reasonable first-order description of the diffraction process.

If one is interested in the extent of the far-field beam, then the corresponding  $\Delta\phi_{0,opt}$  depends on the phase error ( $s = a^2/2\lambda L$ ) across the mouth of the horn. If the phase error is zero then the waist occurs at the aperture, and the far-field beam pattern corresponds to  $\Delta\phi_{0,opt} = \pi/2$ . If there is a finite phase error, the waist is *not* at the aperture, and the far-field power pattern corresponds to a  $\Delta\phi_{0,opt}$  of *less than*  $\pi/2$  [13]. In general, if the beam propagates some distance through a waveguide before reaching the point at which it is truncated, the phase slippage corresponds to the total phase slippage accumulated *since leaving the aperture*. Notice that because  $\Delta\phi_{0,opt}$  is multiplied by an even number when calculating power loss,  $P_t$  will be the same for  $\Delta\phi_{0,opt}$  and  $\Delta\phi_{0,opt} + n\pi$ , where  $n$  is an integer.  $P_t$  is therefore only plotted for values of  $\Delta\phi_{0,opt}$  lying between  $-\pi/2$  and  $\pi/2$ . Strictly speaking only half of the plot is required because the truncation loss is symmetric; conceptually, however, it is easier, when doing calculations, if both halves are visible.

In the case of the uniformly illuminated aperture, it can be seen that there are poorly-defined sidelobes that propagate to high values of  $r/W$  as  $\Delta\phi_{0,opt}$  increases. This structure is real and can be related to the number of Fresnel zones that fill the aperture. A similar structure appears in some of the other plots. It is clear from Fig. 2, that it is almost impossible to transmit the beam from a uniformly illuminated aperture through an optical system: beam spreading occurs even for small values of phase slippage, and away from the near-field region, a significant fraction of the power is diffracted to large values of  $(r/W)$ .

At the other extreme, a corrugated horn only requires  $r_t \geq 2.0W$  for the losses to be less than  $0.035dB$ , or equivalently 0.8%. Fig. 1 confirms the ‘‘rule of thumb’’ that, for a corrugated horn, one has to use optical components that are larger than 3 beam radii. In certain regions of the system, the components can be very much smaller, and our graph quantifies this statement.

## 4 USE OF CONTOUR PLOTS TO DETERMINE POWER LOSS

In the previous section, we described how to plot contours of constant loss as a function of normalized truncation and phase slippage. In this section, we explain how to use these plots to calculate the loss at any plane in a complicated optical system. We suggest the following procedure:

1. Determine the size of the beam at the aperture of the horn that maximises the power in the fundamental mode  $W_{h,opt}$ . For the horns considered in this paper, the options are summarised in Table 1.



Horn type	$W_{h,opt}$
top-hat	0.892a
corrugated conical	0.644a
smooth-wall conical	0.770a
diagonal pyramidal	0.430a

Table 1: The size of the beam at the mouth of the horn that maximises the power in the fundamental mode. For feeds having a circular aperture,  $a$  is the radius of the aperture, whereas for feeds having a square aperture,  $a$  is the sidelength of the aperture.

2. Once  $W_{h,opt}$  is known, the mode set is completely defined, and the position and size of the waist can be calculated from:

$$z_h = \frac{L}{1 + \left(\frac{\lambda L}{\pi W_{h,opt}^2}\right)^2} \text{ and } W(0, W_{h,opt}) = \frac{W_{h,opt}}{\sqrt{1 + \left(\frac{\pi W_{h,opt}^2}{\lambda L}\right)^2}}. \quad (30)$$

We also need the phase slippage between the waist and the aperture:

$$\phi_0(z_h, W_{h,opt}) = \arctan\left(\frac{z_h \lambda}{\pi W(0, W_{h,opt})^2}\right) = \arctan\left(\frac{\pi W_{h,opt}^2}{\lambda L}\right). \quad (31)$$

3. Having calculated the position and size of the waist, propagate the beam through the optical system and calculate the size of the beam at the plane of interest,  $W_{opt}$  [1]. Clearly, one can then calculate the normalised radius of the truncating stop  $r_t/W_{opt}$ . To complete the analysis, we also need the phase slippage between the aperture of the horn and the stop  $\Delta\phi_{0,opt}(z) = \phi_{0,opt}(z) - \phi_{0,opt}(z_h)$ , where  $\phi_{0,opt}$  is the phase slippage between the waist and the stop. If there are intervening optical components, one can calculate the total phase slippage by summing the phase slippages accumulated between each of the focussing elements.

4. Once the normalised radius  $r_t/W_{opt}$  and the phase slippage  $\Delta\phi_{0,opt}$  have been calculated, the appropriate contour plot can be used to determine the truncation loss. Note that if  $\Delta(\phi_{0,opt}) > \pi/2$ , then it should be rescaled by subtracting off an integer times  $\pi$  so that  $\Delta(\phi_{0,opt}) - n\pi$  lies between  $-\pi/2$  and  $\pi/2$ .

## 5 EXAMPLE

As an example, consider the 200 GHz to 900 GHz optical system listed in Table 2 [1-4], where a diagonal horn is coupled to a reflecting antenna through a lens and two off-axis mirrors. The horn is part of a superconducting mixer which is located in a cryostat, and therefore the beam has to pass through a window which must be made as small as possible. In Table 2, we list the phase slippage, normalised truncation radius, co-polar percentage power transmission

component	separation(mm)	W(mm)	$a/W$	$\Delta\phi_{0,opt}$ (deg.)	$P_{co}$ (%)	Loss (%)
virtual waist		1.35		-26		
	3.8					
horn aperture		1.5		0	100.0	
	32					
lens (f=32)		6.5	3.8	52	98.3	1.8
	86					
window (50mm)		5.1	4.9	90	98.1	1.8
	280					
mirror (f=280)		14.1	2.5	-21	97.9	1.6
	280					
image		13.2		0		
	350					
mirror (f=350)		14.7	2.4	25	97.6	1.9
	350					
cass focus		6.3		90		

Table 2: Beam parameters of an optical system comprising a diagonal horn, a lens and two off-axis mirrors. The beam parameters are calculated at 400 GHz. The horn is 19.0mm long and has a 3.5mm square aperture.

from horn through relevant component and the co-polar truncation loss for each of the main optical components.

It is clear from Fig. 2 that, for diagonal horns, it is difficult to clear the beam out to a loss better than 1.5%. If we use the technique described above to calculate the amount of power lost at an individual aperture (and assuming no other truncation loss in the optical system) we arrive at the figures given in the last column. As is clear from penultimate column, it is a mistake, however, to think that if one has a cascade of truncating components, the total loss is simply given by the sum of losses associated with the individual components. Obviously, if the beam does not diffract at any of the apertures, the total loss is determined by the aperture with the greatest loss, since it is not possible to lose power twice by truncating a beam at the same normalised radius twice. If the beam does diffract then power can be lost twice. We can use the truncation contour plots using the above procedure, therefore, as a way of establishing how big an aperture should be in order to avoid truncation.

If one wants to calculate the total loss incurred in a system for which the diffraction at each component is significant, one must calculate how the beam spreads at each of the apertures. This calculation can be done by using the truncation scattering matrix technique described in section 3 to characterise the way in which power is redistributed between modes as the beam passes through each stop [15, 8]. We have used such a scattering-parameter technique to analyse the example optical system. It turns out that the total loss (penultimate column) is, as expected, much less than the sum of the individual losses [9].

In Fig. 5, we use the mode coefficients, phase slippages, and Gaussian radii to reconstruct the beam profiles at a number of different planes. Clearly, in this particular case, the apertures are many wavelengths in diameter, and the beam diffracts only slightly after passing through each stop. Consequently, the first lens after the mixer truncates the beam, and this truncated beam passes all of the way through the optical system without much further interference. From a modal point of view, the first lens is acting as a mode filter which rejects some of the higher order modes. In low noise receivers it is, of course, desirable to reject the high-order modes at low temperatures because then less noise is coupled into the system.

## 6 CONCLUSIONS

We have presented a technique for determining the power loss and diffraction effects that occur when the beam in a beam waveguide is truncated by an axially-symmetric stop. The technique is based on the notion that for a multimode Gaussian beam the scale size of the beam at a plane is characterised by the Gaussian radius, and the intensity distribution of the beam is characterised by the phase slippage. Hence, the loss at a truncating aperture is completely determined by these two quantities also.

The most difficult part of an analysis lies in calculating contours of constant loss as a function of normalised truncation and phase slippage. If, however, the truncating aperture is circular, and the beam is expanded in terms of Associated Laguerre modes, the necessary integration can be reduced to evaluating a recursion relationship. The appropriate scattering matrix for an aperture can also be efficiently calculated using the same approach.

## References

- [1] P. F. Goldsmith, "Quasi-optical techniques at millimeter and submillimeter wavelength." in *Infrared and Millimeter Waves*, vol. 8, No. 9, pp 277-343, 1982.
- [2] R. J. Wylde, "Millimeter-wave Gaussian beam-mode optics and corrugated feed horns," *Proc. Inst. Elec. Eng.*, vol. 131, pt. H, pp 258-262, 1984.
- [3] R. Padman, J. A. Murphy and R. E. Hills, "Gaussian mode analysis of cassegrain antenna efficiency," *IEEE Trans. Antennas Propagat.*, vol. AP-35, pp 1093-1103, 1987.
- [4] J. A. Murphy, "Aperture efficiencies of large axisymmetric reflector antennas fed by conical horns," *IEEE Trans. Antennas Propagat.*, vol. AP-36, pp 570-575, 1988.
- [5] S. Withington and J. A. Murphy, "Analysis of diagonal horns through gaussian-hermite modes," *IEEE Trans. Antennas Propagat.*, vol. AP-40, pp 198-206, 1992.
- [6] D. H. Martin and J. Lesurf. "Submillimetre Wave Optics", *Infrared Physics*, vol. 10, pp 105-109, 1978
- [7] J. W. Lamb, "Quasi-optical coupling of Gaussian beam systems to large Cassegrain antennas," *Int. J. Infrared and Millimeter Waves*, vol. 7, pp 1511-1536, 1986.
- [8] R. Padman and J. A. Murphy, "A scattering matrix formulation for Gaussian beam mode analysis," *Proceedings of the IEE/URSI 7th Int. Conference on Antennas and Propagation*, ICAP, pp 201-204, York (April, 1991).
- [9] J.A.Murphy, S. Withington, and A.Egan, "Mode-conversion at diffracting apertures in millimetre and submillimetre-wave optical systems," accepted for publication in the IEEE Transactions on Microwave Theory Techniques.
- [10] I. S. Gradshteyn and I. M. Ryzhik. "Table of Integrals, Series and Products," Academic Press (London), 1980.
- [11] H. Kogelnik and T. Li. "Laser Beams and Resonators". *Proc. IEEE*, vol. 54, pp 1312-1329, 1966.
- [12] C. Aubry and D. Bittern. "Radiation patterns of a corrugated conical horn in terms of Laguerre-Gaussian Functions," *Electron. Lett.*, vol. 11, pp. 154-156, 1975.
- [13] J. A. Murphy and R. Padman, "Phase centers of horn antennas using Gaussian beam mode analysis," *IEEE Transactions Antennas Propagat.*, vol. AP-38, pp 1306-1310, 1990.
- [14] S. Withington, J. A. Murphy, A. Egan and R. E. Hills, "On the design of broadband quasi-optical systems for submillimetre-wave radio-astronomy receivers," *Int. J. Infrared and Millimeter Waves*, vol.13, pp 1515-1537, 1992.
- [15] P. Belland and J.P. Crenn. "Changes in the characteristics of a Gaussian beam weakly diffracted by a circular aperture." *Applied Optics*, vol. 21, pp 522-527, 1982.

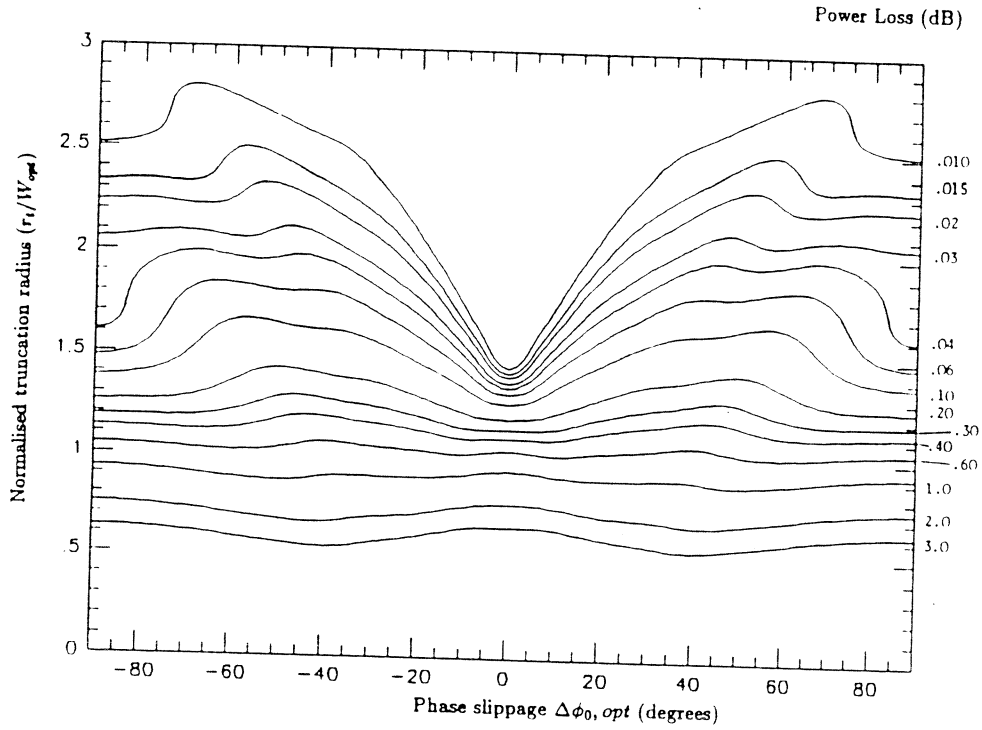


Fig. 1 Contours of constant power loss (dB) as a function of phase slippage and normalised truncation for the beam of a corrugated horn.

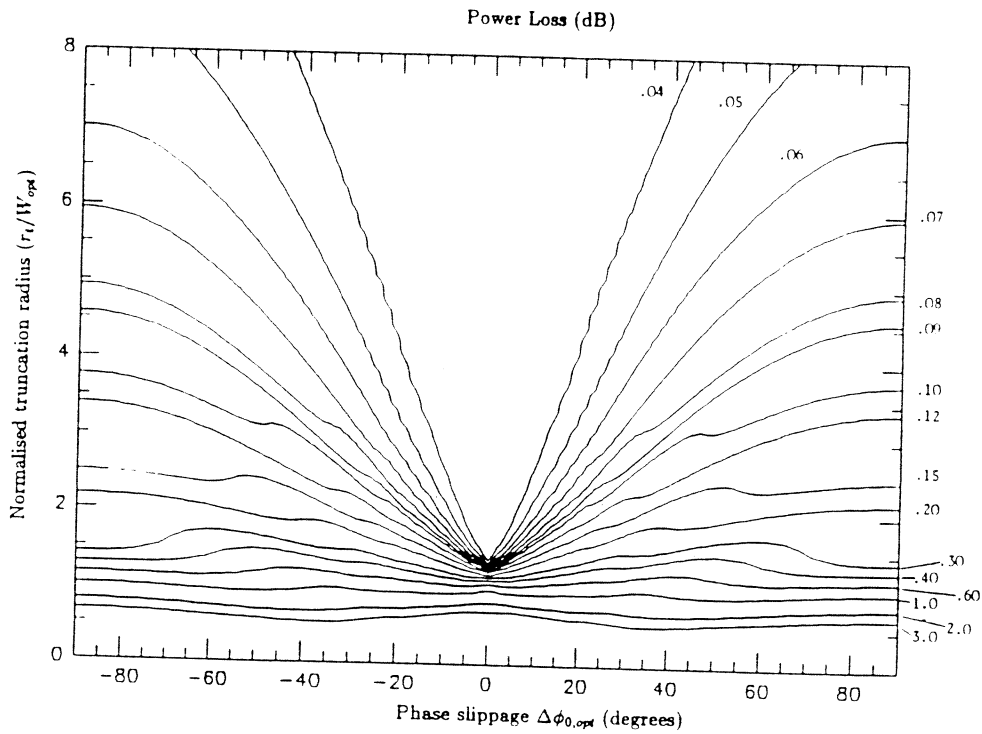


Fig. 2 Contours of constant power loss (dB) as a function of phase slippage and normalised truncation for the co-polar beam of a diagonal horn.

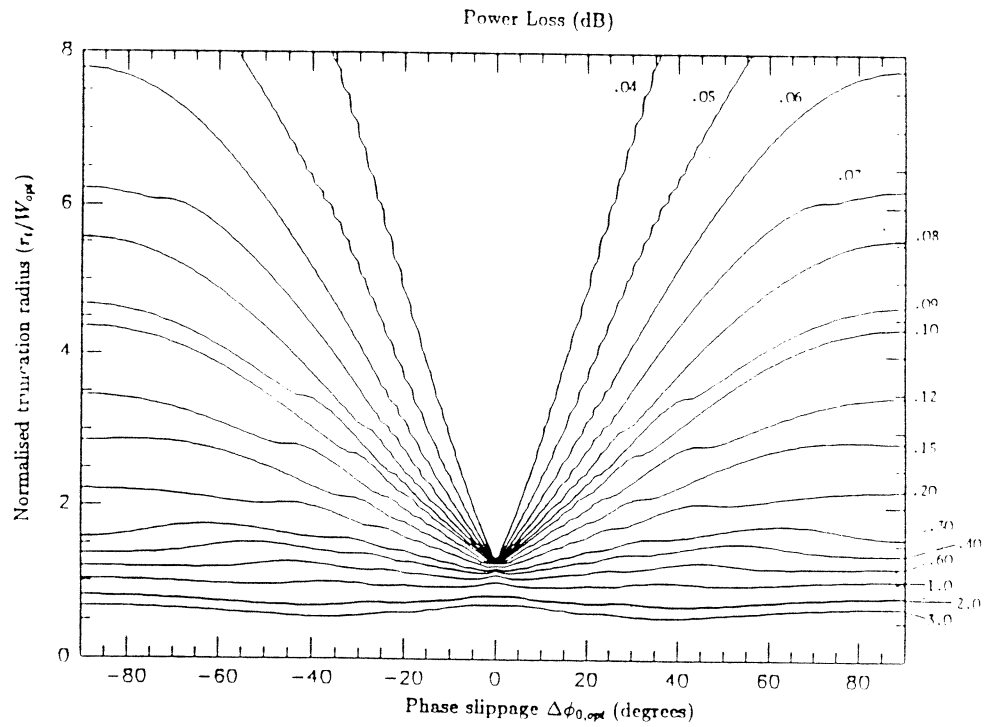


Fig. 3 Contours of constant power loss (dB) as a function of phase slippage and normalised truncation for the *co-polar* beam of a smooth-walled conical horn.

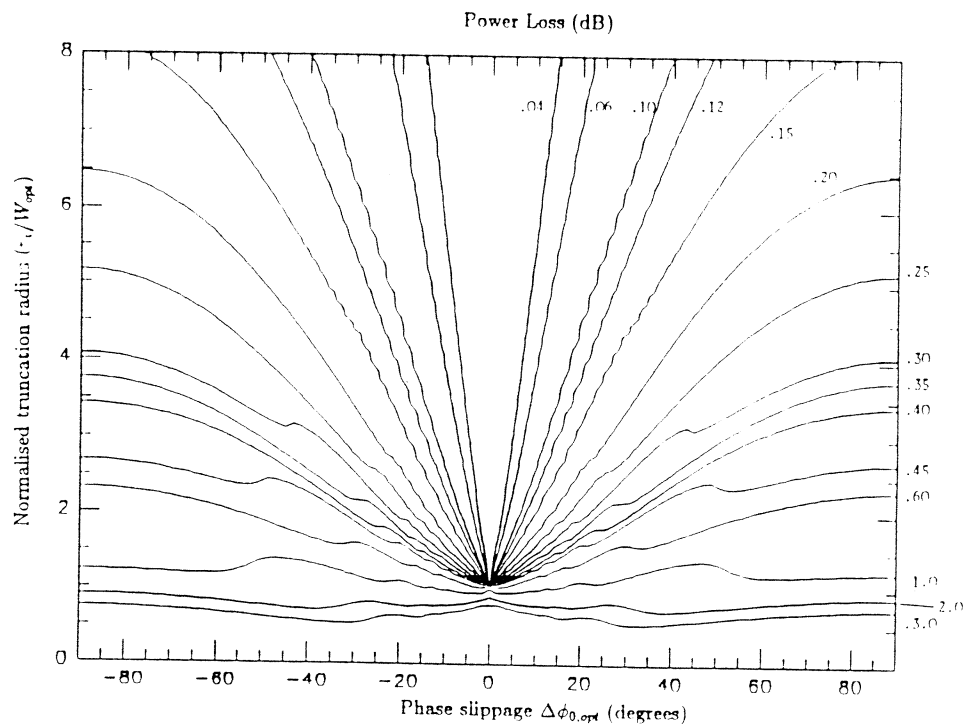
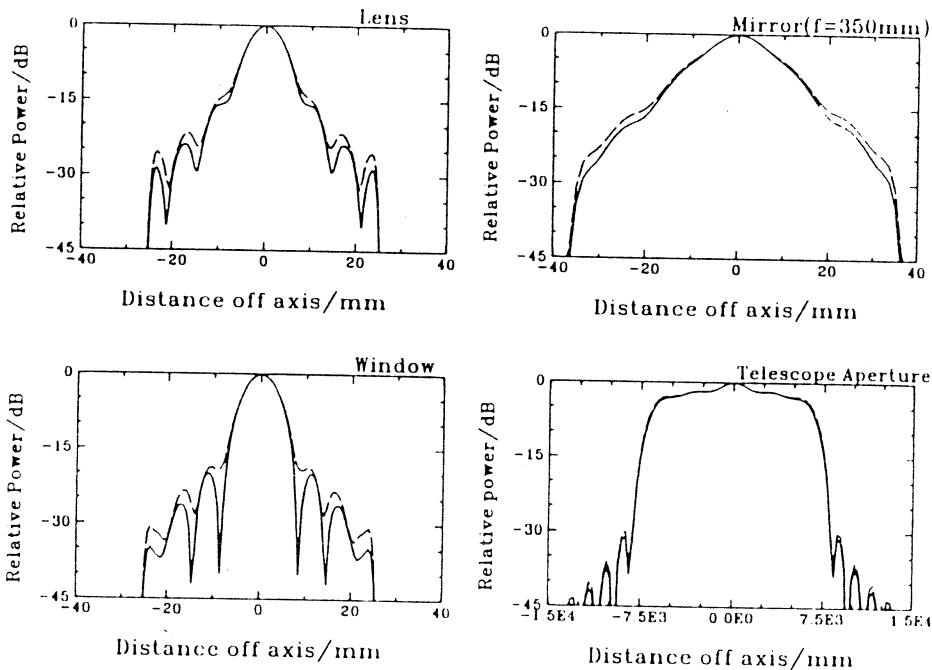
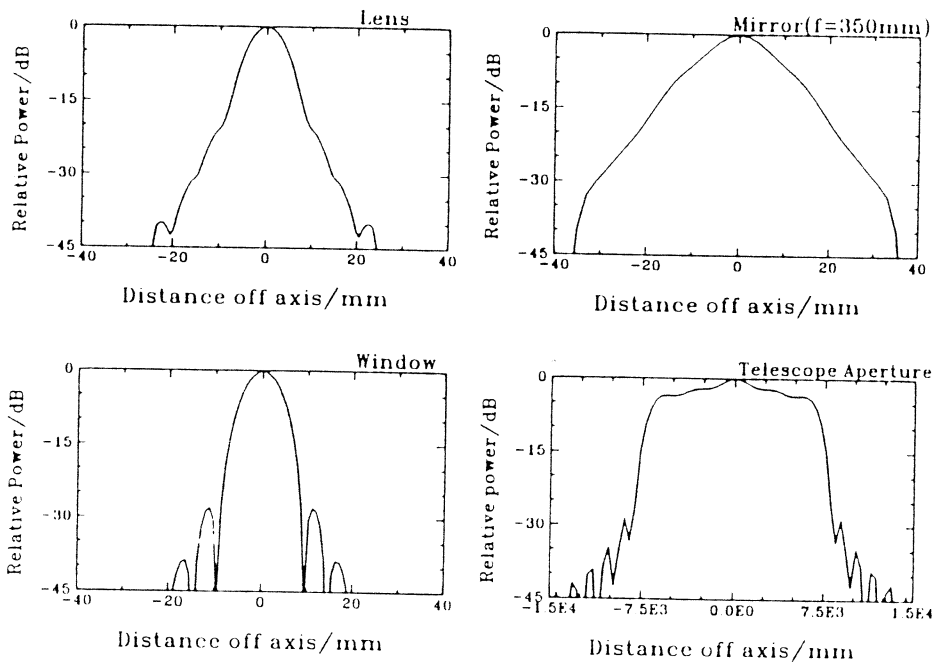


Fig. 4 Contours of constant power loss (dB) as a function of phase slippage and normalised truncation for the beam of a uniformly illuminated aperture.



X-Y Plane Power Patterns



V-H Plane Power Patterns

Fig. 5 Reconstructed beam profiles at various planes in the example optical system . The two curves correspond to the copolar power (solid line) and total power (dashed line). Also